In-Situ Synthesis of Soluble Poly(3-hexylthiophene)/Multiwalled Carbon Nanotube Composite: Morphology, Structure, and Conductivity

Biplab K. Kuila, Sudip Malik, Sudip K. Batabyal, and Arun K. Nandi*

Polymer Science Unit, Indian Association for the Cultivation of Science, Jadavpur, Kolkata 700 032, India

Received July 11, 2006; Revised Manuscript Received November 7, 2006

ABSTRACT: Soluble poly(3-hexylthiophene) (P3HT)−multiwalled carbon nanotube (MWNT) nanocomposites (PCNCs) are prepared by the in-situ oxidative polymerization of 3-hexylthiophene (3HT) in a dispersion of MWNT in $CHCl_3$. The MWNT−P3HT nanocomposite produces blackish-brown solution in chloroform, making it an easily processable system. With increase in MWNT concentration the molecular weight of P3HT has increased, but at higher MWNT concentration (8% w/w) the molecular weight has decreased. The head−tail (H−T) regioregularity of the samples remains the same with that of pure P3HT. The TEM pictures of PCNC-1 and PCNC-8 [the number indicates percentage (w/w) of MWNT with respect to monomer in the composite] show uniform wrapping of MWNT with P3HT. The increase of outer diameter in wrapped MWNT decreases with increase in MWNT concentration, but the PCNC-2.5 exhibits phase segregation by the formation of separate spheroid-like species on the partially wrapped MWNT surface. The higher molecular weight P3HT produced in the PCNC-2.5 has been attributed to this difference in morphology. Type 1 P3HT crystal is formed in all the PCNCs, and melting temperature shows an increase with increasing MWNT concentration except for the PCNC-2.5 sample. The glass transition temperature (T_g) remains unchanged in the PCNCs, but the β-transition temperature (T_β) varies differently in the different PCNCs. The storage modulus of PCNCs has increased abruptly (maximum increase 158%) in the PCNCs than that of pure P3HT. The UV−vis spectra of PCNCs show a red shift in the $\pi-\pi^*$ transition band while the emission spectra show a small blue shift with increase in MWNT concentration. Fluorescence quenching occurs in the PCNCs, and it increases with increase in MWNT concentration except for the PCNC2.5 sample. The conductivity values of both undoped and doped PCNCs have increased significantly with increase in MWNT concentration. FT-IR spectra and NMR spectra indicate the presence of both CH$-\pi$ and $\pi-\pi$ interaction between P3HT and MWNT. Thus, the increased conductivity and mechanical properties of P3HT in the easily processable MWNT−P3HT nanocomposite are interesting for its probable use in different optoelectronic appliances.

Introduction

After its discovery in 1991, carbon nanotubes (CNT) have drawn considerable research interest due to its unique physical, mechanical, and conductivity properties.[1−3] They are classified as single-walled (SWNT) and multiwalled (MWNT) carbon nanotubes depending on the number of folds present in the tube. But they are difficult to process due to its insolubility in most of the solvents. One strategy to overcome this difficulty is the wrapping of carbon nanotube with polymer, which renders them soluble in common solvents.[4−9] This tendency of wrapping of polymer on the wall of CNTs through noncovalent interaction, e.g., $\pi-\pi$ interaction and or CH$-\pi$ interaction, can make CNTs dispersed in the polymers.[10−15] Recently, the direct polymerization of monomers in CNT-dispersed medium through functionalization of CNT has achieved great attention to prepare polymer wrapped CNTs.[8,16−21]

Conducting polymers are important materials because of their applications in the field of sensors, energy storage, corrosion inhibitor, enzyme activity, electronic, and optoelectronic devices. Among its members, poly(3-hexylthiophene) (P3HT) is important because of its solubility and high conductivity.[22,23] The polymer also exhibits a photoluminescence property which can be tuned in its nanocomposite prepared by different procedures.[24,25] The conductivity of this polymer depends on the head−tail (H−T) regioregularity of the chain; the higher the regioregularity, the higher is the conductivity.[26] Further, the conductivity of the P3HT depends on processing condition; e.g., the solvent-cast samples have 1 order higher conductivity than the melt-cooled samples.[26] Again, the spin-coated samples have 2 orders higher conductivity than that of the solvent-cast film.[27] The reason for the former is the presence of network morphology in the solvent-cast film and its absence in the melt-cooled film while the higher conductivity in the spin-coated film than that of the solvent-cast film is due to the higher field effect mobility and homogeneous conjugation.[27]

Recently, both conducting polymer−clay nanocomposites[24,25,28−31] and conducting polymer−carbon nanotube composites[19,21,33−39] are widely studied to make a large scale enhancement in the physical, mechanical, optical, and conducting properties. In the P3HT−clay nanocomposite the conductivity of the nanocomposite remains unaltered, but the storage modulus showed a dramatic increase (770%) in the nanocomposite for clay loading less than 5% (w/w).[24,25] The solvent-cast P3HT−clay nanocomposite exhibits photoluminescence quenching,[24] but the melt-cooled P3HT−clay nanocomposites exhibit enhancement of photoluminescence efficiency with increase in clay content.[25] The multiwalled carbon nanotube (MWNT)−poly(3-octylthiophene) (P3OT) composites prepared by mixing the hexane solution of former with the chloroform solution of latter show a 5 orders increase in conductivity of the composites than that of the pure P3OT. This suggests that there might be some interaction between the MWNT and the

* Corresponding author. E-mail: psuakn@mahendra.iacs.res.in.

10.1021/ma061548e CCC: $37.00
Published on Web 12/22/2006

polymer chains.[39] However, the optical absorption spectra of the P3OT−single-walled carbon nanotubes (SWNT) did not change significantly up to 5 wt % SWNT. This implies that no significant ground-state interaction takes place between the two materials, causing no charge transfer.[38] The dye *N*-(1-pyrenyl)-malemide (PM), functionalized SWNT−P3OT composite showed improved photovoltaic behavior compared to the SWNT−P3OT diode without dye.[37] This has been attributed to the efficient transfer of holes by the dye molecules to P3OT at the dye−polymer interface and rapid transfer of generated electrons to the SWNTs at the dye−nanotube interface. In the SWNT−poly-(ethylene dioxythiophene) (PEDOT) composites, the electroluminescence, current (*I*)−voltage (*V*) data, and photoluminescence suggest an electronic interaction between SWNT and PEDOT; the electronic interaction originates from the hole-trapping nature of SWNT in a hole-conducting polymer.[40]

Thus, from the above discussion it is apparent that poly(3-alkylthiophene) (P3AT)−CNT nanocomposites exhibit interesting physical, optical, and conductivity properties, but the reason for such improvement is not clearly understood. For a fruitful use of the properties a clear understanding of the behavior of the P3AT−CNT nanocomposite prepared from different techniques is necessary. Here we report the in-situ preparation and properties of MWNT−poly(3-hexylthiophene) (P3HT) nanocomposite without functionalization of MWNT. No report has yet been made for the in-situ preparation of the MWNT composites of the P3ATs, and it is the first time report in this P3AT system. We want to explore how the molecular weight, polydispersity, and regioregularity of P3HT vary with MWNT concentration during the in-situ polymerization using $FeCl_3$ as initiator. The influence of MWNT on the mechanical properties of P3HT is interesting to study for its probable use in different optoelectronic appliances. Further, because of the difference of pendent alkyl chain length between P3HT and P3OT, some difference in physical properties of the two composites is expected.[26,41] In this article the morphology, structure, thermal properties, optical properties, and conductivity are reported for these composites with varying MWNT concentration. A probable explanation of the difference in physical properties of the composites with different MWNT concentration is also presented here.

Experimental Section

(a) Preparation of the Nanocomposite. MWNTs were purchased from Aldrich Chemical Co. [product no. 636495, lot no. 04619DC, produced by the chemical vapor deposition (CVD) method]. The Raman spectrum of the MWNT sample (excitation wavelength 632.8 nm with a procedure reported elsewhere)[42] is presented in Figure 1, where the D and G bands are clearly observed. The D band is around 1319 cm^{-1}, and it is intense while the G band has a doublet around 1563 and 1588 cm^{-1}. The former band characterizes the disorder-induced phonon mode due to infinite size of crystals and defects while the latter bands characterize the Raman-allowed phonon mode (E_{2g}) of the graphite ring (sp^2 carbon).[43] The1588 cm^{-1}peak of the doublet might arise due to the splitting of the degenerate E_{2g} state or from the existence of a different energy state.[43] So the Raman spectra indicate that the MWNT sample has a low degree of graphitization.[44,45] P3HT was prepared in the laboratory from the monomer 3-hexylthiophene (Aldrich Chemical Co.) by oxidative polymerization using $FeCl_3$ as initiator in $CHCl_3$ medium[46] where MWNTs were dispersed at different concentrations. The MWNTs concentrations were chosen as 1%, 2.5%, and 8% (w/w) with respect to monomer (0.336 g), which was sonicated in an ultrasonic bath (60 W, model AV10C, Eyela). Anhydrous $FeCl_3$ (1.3 g) was dispersed in 100 mL of dry $CHCl_3$ by stirring at 10 °C for 12 h. The MWNT mixed monomer solution was then gradually mixed with the initiator solution at 0 °C. The polymerization was carried out at 0 °C for 24 h, and the reaction mixture was poured into methanol containing 10% (v/v) 12 N HCl. The precipitate was washed with methanol and dried in vacuum at 60 °C.

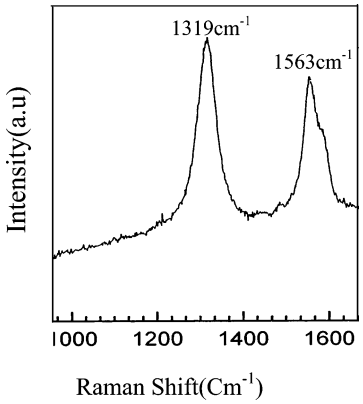

Figure 1. Raman spectrum of MWNT sample for excitation at 632.8 nm.

The as-prepared MWNT−P3HT nanocomposites and pure P3HT when dissolved in $CHCl_3$ contain some insoluble matter. So the solution was sonicated, filtered, and dried. The dried sample was then used to measure the head−tail regioregularity by proton NMR spectroscopy by dissolving in $CDCl_3$.[46] For measurement of the molecular weight, the PCNC solutions in $CHCl_3$ were centrifuged at 14 000 rpm for 30 min when the MWNTs become detached from the polymer and separated out. The solution was then decanted, and the process was repeated four times to remove the MWNT completely. It was then dried, and the molecular weight was measured using GPC in THF solution at 30 °C. Polystyrene was used as a standard for molecular weight measurement.

(b) Electron Microscopy. The dispersity of carbon nanotubes in the polymer matrix was studied using a transmission electron microscope (TEM JEOL, 2010EX) operated at an accelerated voltage of 200 kV. A drop of dilute solution of the composite in ethanol dispersed by sonication on the carbon-coated copper grid was dried finally in vacuum and was directly observed in the TEM. The EDXS experiment on the selected portion of the sample was made using INCAx-sight (Oxford Instruments) operated with INSA suite software (version 4.02).

For the SEM study a dried film of the composites was platinum coated and was observed through a field emission scanning electron microscope (JEOL GSM-5800) at 2 kV.

(c) Wide-Angle X-ray Scattering (WAXS). The WAXS experiments were carried out on the solvent-cast films of the MWNT−P3HT (in-situ) nanocomposite using a Seifert X-ray diffractometer (C3000) in reflection mode with a parallel beam optics attachment. The instrument was operated at a 35 kV voltage and a 30 mA current and was calibrated with a standard silicon sample. Nickel-filtered copper Kα radiation ($\lambda = 0.154$ nm) was used in the work. The samples were scanned from $2\theta = 2°$ to 30° at the step scan mode (step size 0.03°, preset time 2 s), and the diffraction pattern was recorded using a scintillation counter detector.

(d) Thermal Study. The melting point and enthalpy of fusion data of the MWNT−P3HT nanocomposites (in-situ) were measured by a Perkin-Elmer differential scanning calorimeter (Diamond DSC-7) working under N_2 atmosphere. It was calibrated with indium before each set of experiment. About 3 mg of sample was taken in aluminum pans and was crimped by a universal crimper. They were then heated at the scan rate of 10 °C/min from −30 to 230 °C. The melting temperature and enthalpy of fusion were measured with the help of a personal computer using Pyris software (version 7.0). The reproducibility of DSC peak positions for repeated measurements is within 0.1 °C.

The thermal stability of the PCNCs was measured using a Perkin-Elmer TGA Instrument (Pyris Diamond TG/DTA) under a nitrogen atmosphere at a heating rate 10 °C/min.

Table 1. Characteristics of P3HT Sample Produced during in-Situ Polymerization with MWNT at 0 °C

concn of MWNT with respect to monomer ((w/w) %)	mol wt ($\bar{M}_w$) $\times 10^{-5}$	PDI	H−T regioregularity (mol %)	melting point (°C)	enthalpy of fusion (J/g)
0	1.11	1.78	81	197.0	6.1
1	1.65	2.07	82.7	197.8	6.9
2.5	2.02	2.1	82.5	196.8	8.3
8	0.7	2.10	82.2	199.5	11

(e) Spectral Characterization. The FTIR spectra of the samples were performed from a KBr pellet of the nanocomposites in a Shimadzu FTIR instrument [FTIR-8400S SHIMADZU]. The UV−vis spectra of the MWNT−P3HT composites (in-situ) were made by casting the film on quartz plate. The spectra were taken against air at 30 °C in a UV−vis spectrophotometer (Hewlett-Packard, model 8453) from 200 to 1000 nm. The photoluminescence experiments of the solvent-cast films of the in-situ nanocomposites were performed on a Perkin-Elmer instrument (LS55 luminescence spectrometer). The photoexcitation was made at an excitation wavelength of 490 nm at a 45° angle of the thin film plane of the sample with the excitation beam. The emission was detected at a right angle to the excitation beam direction. Each spectra was normalized for 1 μm film thickness for comparison purposes.

(f) Dynamical Mechanical Property Measurement. The storage modulus, loss modulus, and tan δ properties of the in-situ MWNT−P3HT nanocomposites were measured using a dynamical mechanical analyzer (DMA) (TA Instruments, model Q-800). Films of 25 mm × 5 mm × 0.15 mm dimension were made from composite solution by casting on a die, and they were installed in the tension clamp of the calibrated instrument. The samples were heated from −130 to 150 °C at a heating rate of 10 °C/min. The storage modulus, loss modulus, and tan δ were measured at a constant frequency of 10 Hz with a static force of 0.02 N.

(g) Conductivity Measurement. The dc conductivity of in-situ MWNT−P3HT nanocomposite films were measured at 30 °C using the standard spring loaded, pressure contact, four-probe method. A circular film of 1.3 cm diameter was used, and the probe was connected with the help of Ag paste. A constant current (I) was passed from a dc source electrometer (Keithley model 617) through two diagonal leads, and the voltage was measured using a multimeter (Keithly, model 2000). The conductivity was calculated from the relation

$$\sigma = (\ln 2/\pi d)(I/V) \quad (1)$$

where d is the thickness of the film which was measured by a screw gauge, averaged to four measurements at different places of the film. Conductivity of two films each with two trials was measured and the average of four such measurements were taken as the conductivity of the samples. Iodine-doped samples were prepared by exposing the film over iodine vapor for 24 h, and the conductivity was measured by the standard four-probe method.

Results and Discussion

Characteristic of P3HT. The MWNT−P3HT nanocomposite produces blackish-brown solution in chloroform, making it an easily processable system. The characteristics of P3HT produced during the in-situ preparation of MWNT−P3HT nanocomposite are presented in Table 1. The molecular weight is reported here after the removal of carbon nanotube by repeated centrifugation at 14 000 rpm, and during the centrifugation the MWNT become separated from the polymer. This is because the polymer chain experiences different torque than the higher weight carbon nanotube ($\sim 8 \times 10^5$) separating the two which were attached by weak physical forces (e.g., CH−π and/or $\pi-\pi$ interactions).[14,38,47] It is important to note from Table 1 that the molecular weight of P3HT has increased for 1% and 2.5% MWNT concentration, but for 8% concentration it decreases substantially. No definite reason for this behavior is known, and it might be possible for the attachment of the monomer on MWNT surface by $\pi-\pi$ and/or CH−π interactions.[14,47] The initiation starts on the bound monomer molecules, from where the chain propagates. Because of the attachment of the growing polymer chain with the MWNT, the degree of freedom of the chain decreases. As a result, the termination by combination of the propagating chain decreases, causing a higher molecular weight. At 2.5% MWNT concentration the molecular weight is highest probably because of increased concentration of the bound monomer which decreases the termination rate by combination or chain transfer processes. But an increase of 8% concentration of MWNT in the medium causes some free MWNT, which deactivates the propagating chain radical by a transfer mechanism, decreasing the molecular weight abnormally. Thus, it may be argued that at the 2.5% concentration the whole surface of MWNT may be totally filled by the monomer molecules, giving an optimum condition for producing the highest molecular weight polymer. The polydispersity index of the polymer in MWNT−P3HT composites is the same for three different systems, but it is higher than that of pure P3HT. The reason may be due to the termination at various stages of propagating chain in the composites. The head−tail regioregularity measured from proton NMR was found to be the same in the nanocomposite as well as in the pure polymer. The melting point (T_m) and enthalpy of fusion values of the in-situ prepared composites increases with increase in MWNT concentration.

Morphology. In Figure 2 the SEM pictures of MWNT, PCNC-1, PCNC-2.5, and PCNC-8 are shown. The MWNTs have tubular network structure both in the pure state and in the composites. It is important to note that the MWNTs are fatter in all the PCNCs than those in the pure sample. However, PCNC-1 and PCNC-2.5 tubes are fatter than that of PCNC-8. The reason may be due to the fact that MWNTs are wrapped better by the polymer in PCNC-1 and PCNC-2.5 than that in PCNC-8. Also, some spheroid-like morphology is observed on the surface of the MWNT of PCNC-2.5. To ascertain the physical nature of the MWNT in the composite more clearly, the TEM pictures of MWNT and the composites are presented in Figure 3a−d. The MWNT tube has outer diameter 13-23 nm, and the inner diameter is about 7−15 nm. The length of MWNT varies from 0.5 to 2 μm as mentioned by the company. From Figure 3b it is apparent that the MWNTs of PCNC-1 have a thicker outer diameter ($\sim$78 nm) than that of the pure sample. This is also true for other composites; e.g., for PCNC-2.5 the average outer diameter is $\sim$50 nm, and for PCNC-8 it is $\sim$42 nm. Thus, from the increase of thickness of outer diameter it can be inferred that MWNTs are wrapped well by P3HT, and larger the concentration of MWNT, the lower is the degree of wrapping. The wrapping of MWNT may be directly evidenced from a EDXS spectrum for the PCNC-1 composite (Figure 4). Here the presence of both carbon and sulfur on the wall of the nanotube is evidenced from the peak of carbon and sulfur. This study therefore concludes that during the in-situ polymerization of 3-hexylthiophene in the MWNT dispersion in $CHCl_3$ the surface of MWNTs is well wrapped by the P3HT. The inset of Figure 3b presents enlarged image of the marked portion. This figure clearly put a evidence that the darker contrast MWNT is wrapped by the lighter contrast P3HT. A critical survey of the

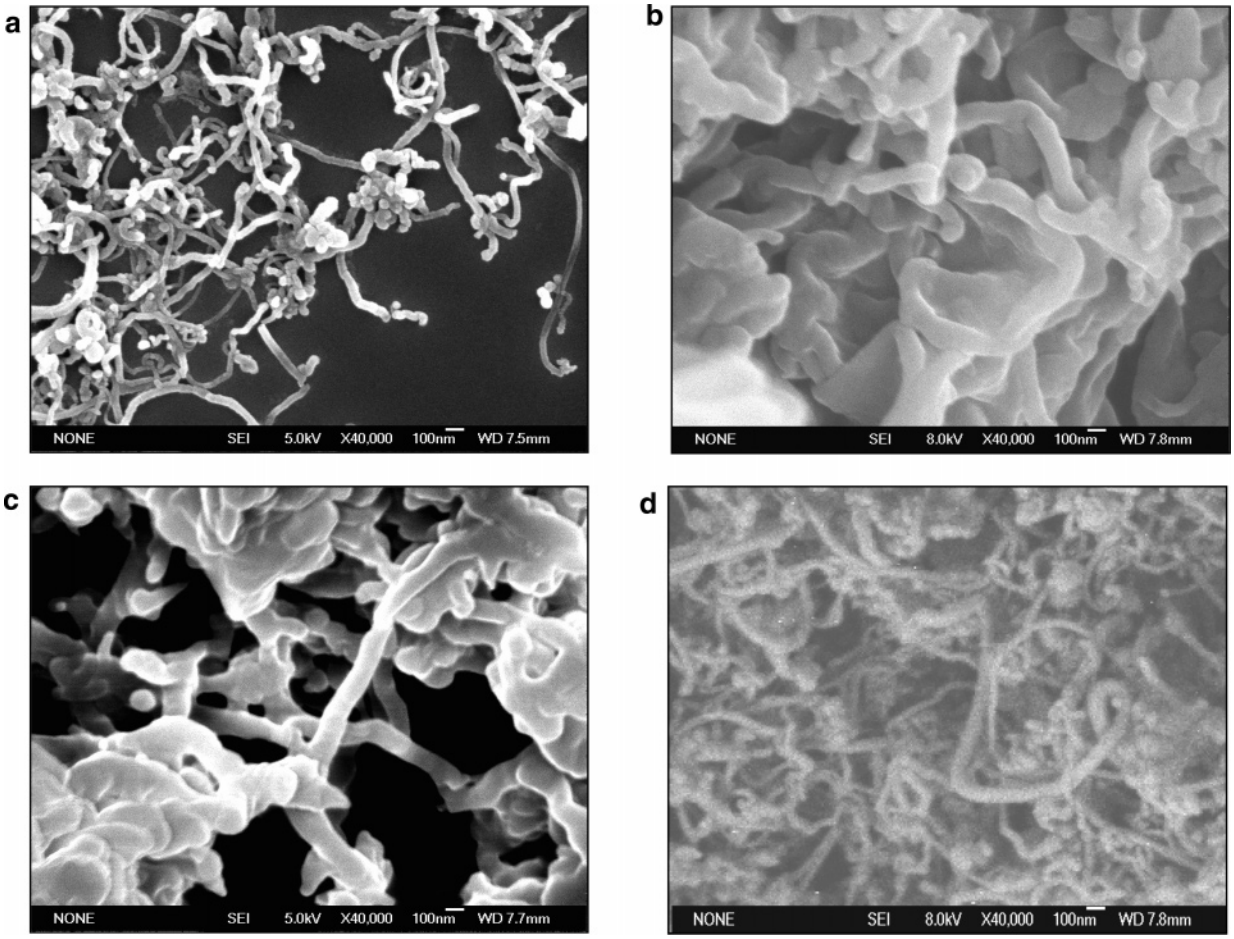

Figure 2. FE-SEM picture of (a) MWNT, (b) PCNC-1, (c) PCNC-2.5, and (d) PCNC-8.

TEM pictures of Figure 3a−d indicates that the morphology is not similar in all the cases. In Figure 3a,b,d the surface of the nanotubes is smooth, but in Figure 3c the surface of the nanotubes is full of protuberance. These spheroid-like particles on the nanotube surface (also seen in SEM picture (Figure 2c)) indicate that the P3HT produced at this composition does not wrap the MWNT fully. Some portions of it remain phase separated, producing spheroid-like particles (see also Figure 1 of the Supporting Information at higher magnification). The only difference between this sample and the other P3HTs produced in-situ is the highest molecular weight of this sample (Table 1), and it might be possible due to this molecular weight difference such an inhomogeneous mixing results.

Wide-Angle X-ray Scattering. In Figure 5 the WAXS patterns of MWNT, P3HT, PCNC-1, PCNC-2.5, and PCNC-8 are presented. From the figure it is apparent that MWNT has diffraction peak at $2\theta = 26°$, corresponding to the *d* value of 3.42 Å, for the 002 reflection of graphite.[19] On the other hand, P3HT has an interchain lamella peak corresponding to *d* spacing 17.1 Å ($2\theta = 5.2°$) and another diffraction peak corresponding to intrastack chain-to-chain repeat distance of 3.78 Å ($2\theta = 23.2°$). The X-ray diffraction pattern corresponds to the type I crystal of P3HT,[48−50] and on addition of MWNT the polymorphic nature of P3HT remains unchanged. In the composites the intensity of the characteristic 002 reflection of MWNT increases with increasing concentration of MWNT, and in PCNC-8 this peak is very prominent.

Thermal Behavior. In Figure 6 the DSC thermograms of P3HT and different PCNCs are compared. The melting points of P3HT, PCNC-1, PCNC-2.5, and PCNC-8 are 197.0, 197.8, 196.8, and 199.5 °C, respectively, indicating that the melting point of the P3HT has increased in the PCNCs except for the PCNC2.5 sample. The enthalpy of fusion (ΔH) values are 6.1, 6.9, 8.3, and 11.0 J/g for P3HT, PCNC-1, PCNC-2.5, and PCNC-8, respectively. The reason for this increase in enthalpy of fusion and melting point is unknown, and it might be possible that MWNTs influence the P3HT coils to organize in a more ordered manner. The lower T_m value of PCNC-2.5 indicates that the organizing influence of MWNT is not operating here.

Thermogravimetric Analysis. The TGA thermograms of P3HT and the PCNCs are presented in Figure 2 of the Supporting Information. The P3HT, PCNC-1, PCNC-2.5, and PCNC-8 exhibit degradation temperature (onset of inflection) at 460, 455, 455, and 457 °C, respectively. These results indicate that the PCNCs have lower thermal stability than that of pure P3HT. However, this is not reflected in the residual weight measured at 800 °C, where the PCNCs with higher MWNT concentration has higher residual weight except for the PCNC-1 sample. The higher residual weight is due to the presence of undegradated MWNTs which usually starts degradation at and above 800 °C.[34,50] Also, it may be noted here that the P3HT has ∼25% residual weight left even heating to 800 °C, so the residual weight in the PCNCs is a mixture of residue of both P3HT and PCNCs. The small decrease in residual weight of PCNC-1 than that of P3HT may be due to the catalytic effect of MWNT for degradation which is manifested in the lower value of degradation temperature.

Mechanical Properties. Figure 7a−c shows the temperature dependency of storage modulus, loss modulus, and tan δ plot of P3HT and of three PCNCs. The storage modulus or elastic modulus (G') relates the ability of the material to store or return energy when an oscillatory force is applied to the sample, and

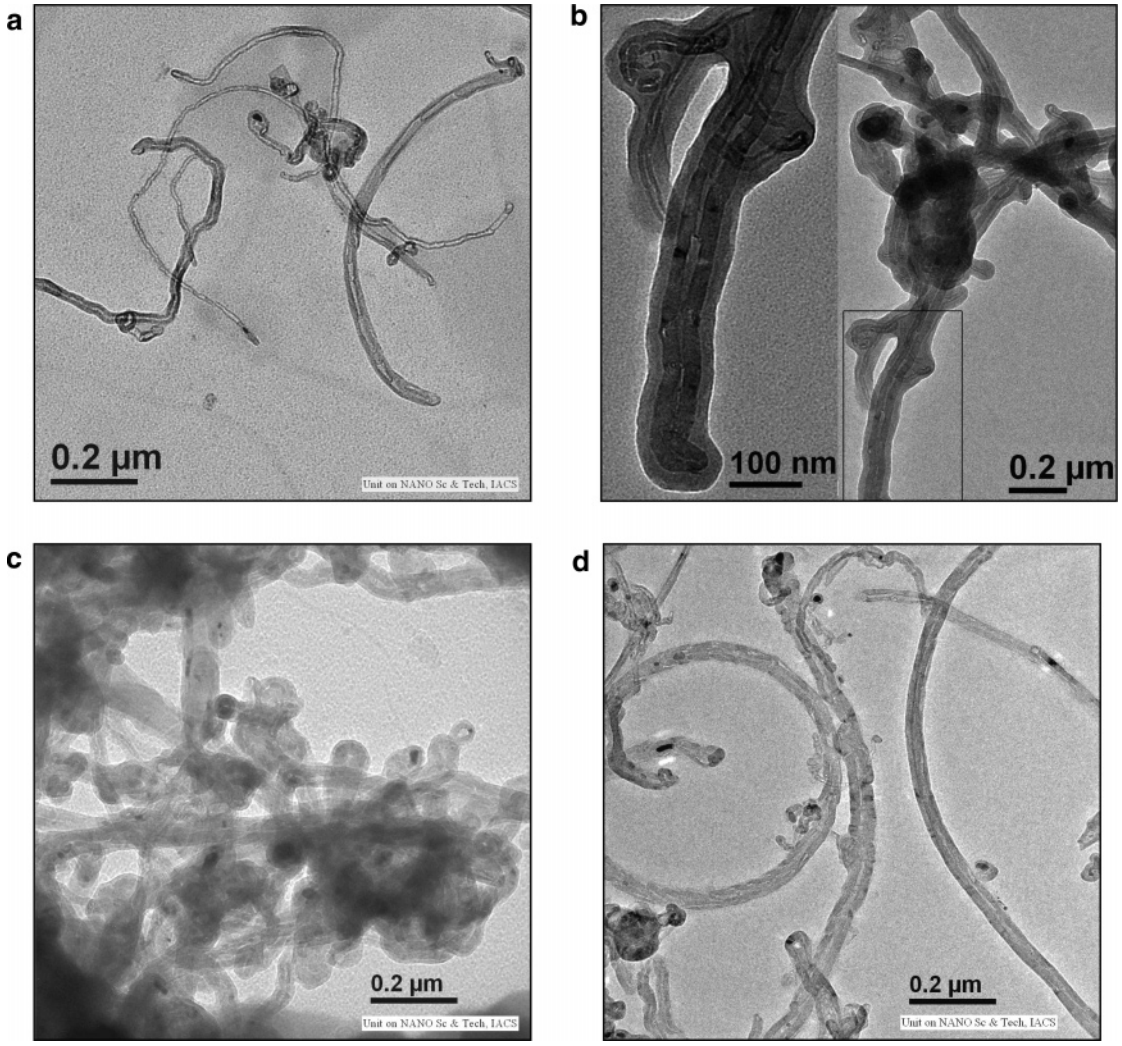

Figure 3. TEM micrographs of P3HT−MWNT nanocomposites: (a) MWNT, (b) PCNC-1 (inset: magnified part of wrapping MWNT), (c) PCNC-2.5, and (d) PCNC-8.

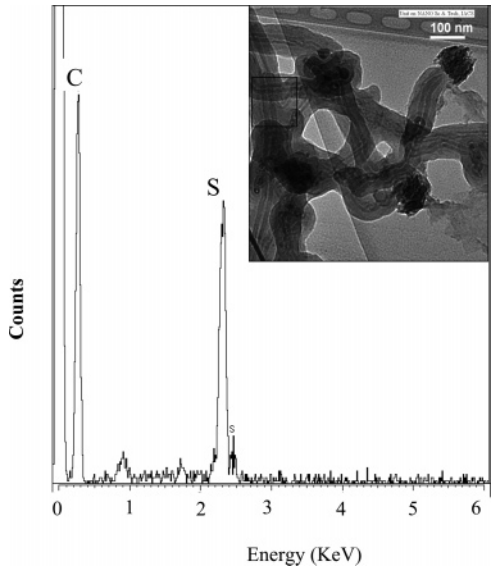

Figure 4. EDXS spectra of the marked portion of PCNC-1.

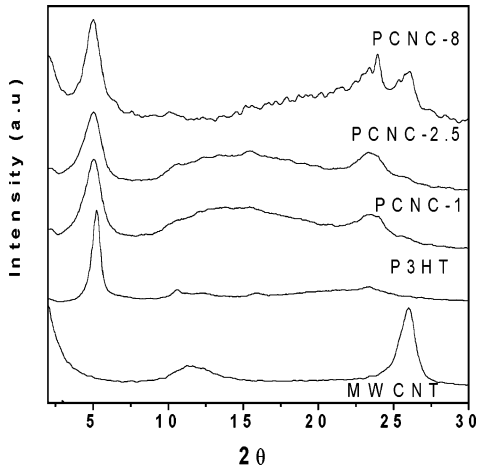

Figure 5. WAXS patterns of P3HT and PCNCs.

the loss modulus (G'') relates the ability to lose the energy. Figure 7a illustrates that with increase in temperature the storage modulus of all the samples decrease, and at about 50 °C it is negligibly small. However, the decrease is not linear, and it exhibits two breaks: one at lower temperature range (∼−90 °C) and the other at higher temperature range (∼20 °C). These two breaks are indication of two different types of transitions which are clearly manifested in the loss modulus temperature plot (Figure 7b) showing two peaks. The lower temperature peak may arise for the β transition (T_β) where relaxation of hexyl side chains of P3HT occurs, and the higher temperature peak (α-transition) arises for segmental relaxation

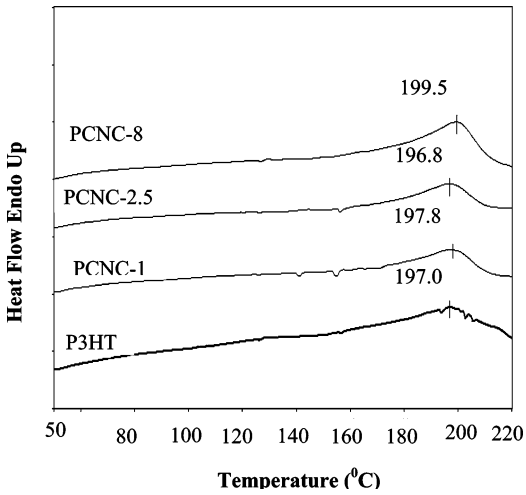

Figure 6. DSC thermograms of the P3HT−MWNT nanocomposites at the heating rate of 10 °C/min.

of the main chain.[24,25,52] The latter transition may be called the glass transition temperature (T_g) of the polymer. In the tan δ vs temperature plot (Figure 7c) there are a broad peak at lower temperature and a sharp peak at higher temperature regions. The former peak temperature may correspond to the T_β, and the latter peak temperature may be the T_g. There is a large difference (e.g., 16−20 °C) between the T_g values measured by loss modulus peak tan δ peak, and similar is the case for the T_β values. The reason for this large difference in the transition temperatures obtained from the loss modulus and tan δ plots is not yet clear to us and might be due to the two different modes of measurement; one is related to the dissipation of energy as heat (loss modulus), and the other is related to the reduction of vibration of the material, i.e., damping (tan δ). A comparison of the storage modulus and loss modulus plots of P3HT and PCNCs suggests that both storage modulus and loss modulus values are higher in the PCNCs than that of pure P3HT, except for the PCNC-8 where the loss modulus has lesser value at low temperature (≤0 °C). This indicates that the causes of increased storage modulus and loss modulus in the PCNCs are almost the same.

To get a clearer picture of the increase of storage modulus in the PCNCs compared to that of pure P3HT, the data are presented in Table 2 for three different temperatures together with their T_β and T_g values. It is apparent from the table that the T_g values remain the same with MWNT concentration of the nanocomposite. But the T_β exhibits a peculiar behavior with MWNT composition as is apparent from Table 2 (inset of Figure 7b). PCNC-1 has higher T_β values than that of pure P3HT, indicating the relaxation process of the hexyl group occurring through bond rotation is hindered. PCNC-2.5 exhibits two T_β values, e.g., −96.9 and −86.1 °C, and might be attributed to two types of P3HT in the system (cf. morphology). The T_β value of −86 °C may be attributed to wrapped P3HT and −96.9 °C to the free P3HT (spheroidal). For the PCNC-8 sample one would therefore expect a higher T_β value than that of pure P3HT; instead, we obtain the same T_β value as in pure P3HT. No definite reason is known, and it might be due to the balance of attractive forces from different directions on the hexyl chains for the larger concentration of MWNT.

A comparison of the storage modulus values of the PCNCs suggest that the percentage increase of storage modulus with increase in temperature increases except for PCNC-2.5, which shows an abnormal decrease at 50 °C from that of 20 °C. At −50 and +20 °C this composite (PCNC-2.5) has the highest increase than that of the other two PCNCs. This comparative higher increase may be due to the separate phase (spheroid-like) present in the PCNC-2.5. But it shows a large decrease at the 50 °C temperature region. No definite reason for this behavior is known, and probably a change of microstructure of this composition may occur at this temperature. Here it is worth comparing the percentage increase of storage modulus values with that P3HT−MMT clay nanocomposite prepared by the solvent-cast method.[24] The highest increase observed in that case was 774%, whereas the highest increase in this case is 158%. Thus, the P3HT−clay nanocomposite has at least 5 times greater reinforcing property than that of the MWNT−P3HT nanocomposite, probably due to the smaller dimension of the clay tactoids (thickness ∼1 nm and length ∼218 nm) than that of MWNT.

Optical Properties. (a) UV−Vis Absorption Spectra. The UV−vis absorption spectra of P3HT and PCNC films are presented in Figure 8. Pure P3HT shows an absorption band at 505 nm corresponding to the $\pi-\pi^*$ transition of its conjugated segments. On addition to MWNT this band gradually shifts toward the higher wavelength region. This is contrary to the usual blue shifts observed in the P3HT−clay[24,25] and P3HT−CdS nanocomposite.[54] Probably the interaction of P3HT on the carbon nanotube surface uncoils the P3HT chain, increasing its conjugation length. This interaction therefore causes a red shift in the UV−vis absorption spectra, and it is the highest for PCNC-8 sample. However, in the poly(3-octylthiophene)−single-walled carbon nanotube (P3OT−SWNT) composite, preparation by simple blending of P3OT and SWNT solution in chloroform does not exhibit any significant change in UV−vis spectra up to 5% SWNT concentration, as reported in earlier work.[38] It might be possible the P3OT do not mix well with the SWNT in the mechanical mixing process due to the lack of specific interaction between the components. But in the in-situ polymer formation on MWNT surface, the monomer molecules become adsorbed on the MWNT surface through physical interaction, and after polymerization this interaction persists (cf. Discussion), increasing the conjugation length of the polymer.

(b) Photoluminescence Spectra. P3HT has a photoluminescence property,[24,25] and the photoluminescence spectra of P3HT and PCNC films, normalized to its thickness, are presented in Figure 9. For an excitation wavelength of 490 nm the films show an emission at 653, 649, 652, and 651 nm for P3HT, PCNC-1, PCNC-2.5, and PCNC-8, respectively. Here the PCNCs also exhibit a photoluminescence quenching except for the PCNC2.5 samples. The reason for the photoluminescence quenching of PCNCs may be due to the $\pi-\pi$ interaction of

Table 2. Summary of Mechanical Properties of PCNCs Measured by DMA

			storage modulus (MPa)					
sample	T_β[a] (°C)	T_g[a] (°C)	−50 °C	(%) increase	20 °C	(%) increase	+50 °C	(%) increase
P3HT	−94.4	28.9	1605		723.7		75.31	
PCNC1	−87	28.7	1989	24	910	26	115.5	53
PCNC2.5	−96.9, −86.1	28.8	2223	39	1061	47	93	24
PCNC8	−96.4	28.2	1900	18	974	35	194.7	158

[a] From loss modulus peaks.

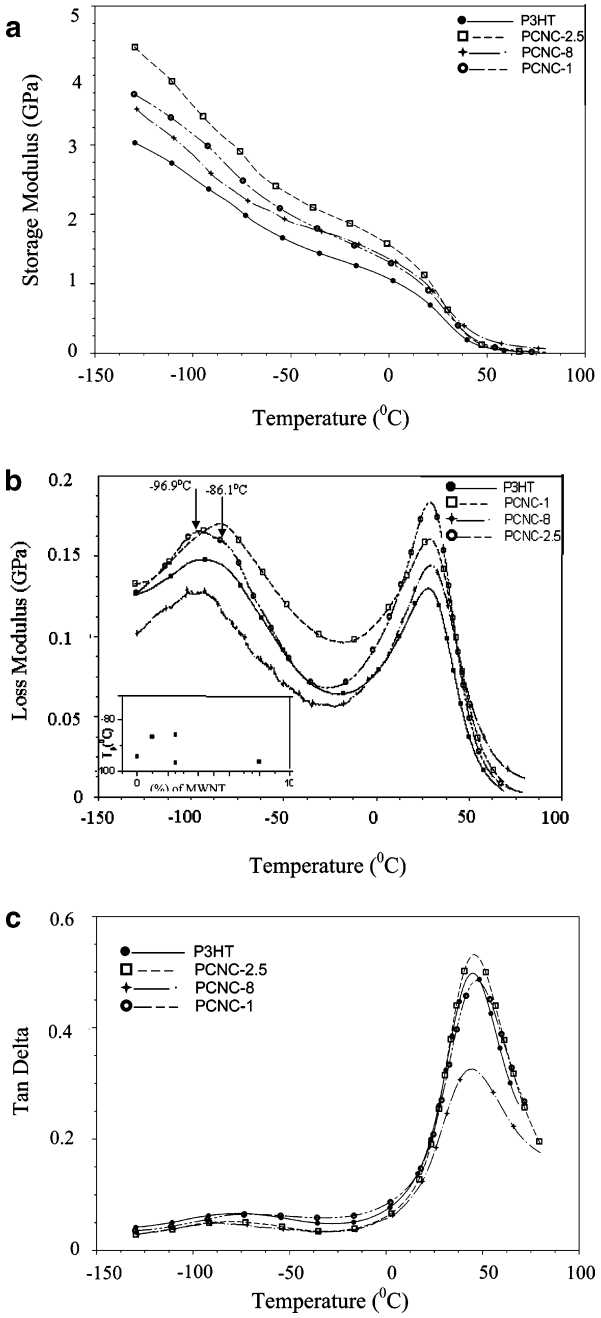

Figure 7. Mechanical property variation of P3HT−MWNT nanocomposites with temperature: (a) storage modulus; (b) loss modulus (inset: T_β with MWNT concentration); (c) tan δ.

P3HT with MWNT,[11] forming additional decaying paths of the excited electrons through the MWNTs, and the greater the concentration of MWNTs, the larger is the photoluminescence quenching. The almost unperturbed photoluminescence property of the PCNC-2.5 (Figure 9) is probably due to the microphase separation of the P3HT in the composite. The small blue shift in the nanocomposite emission spectra indicates that the ground state energy level is more stable in the nanocomposites than that of pure P3HT. This may be possible through the resonance stability of π clouds of P3HT and graphite units of MWNT through $\pi-\pi$ interaction (cf. Discussion).

Conductivity. The dc conductivities of P3HT and the PCNCs measured at 30 °C are presented in Table 3 for both undoped and iodine-doped samples. It is apparent from the table that the conductivity of PCNCs increases with increase in MWNT concentration for both the undoped and I_2-doped state. In the

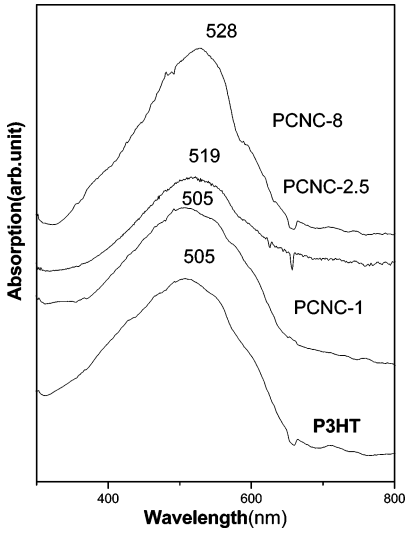

Figure 8. UV−vis absorption spectra of P3HT and PCNC films at 30 °C.

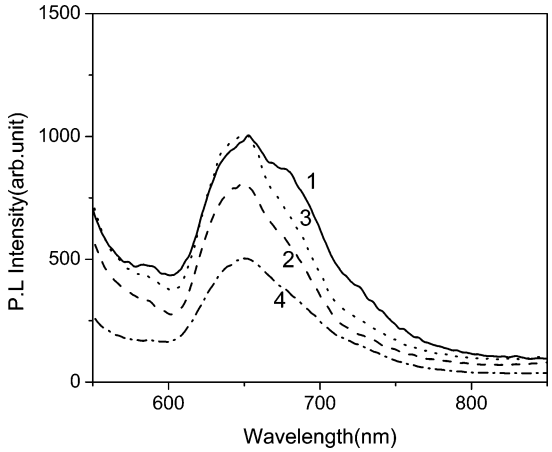

Figure 9. Photoluminescence spectra of P3HT−MWNT nanocomposites after excitation by radiation of 500 nm wavelength (normalized to film thickness of 1 μm): 1, P3HT; 2, PCNC-1; 3, PCNC-2.5; 4, PCNC-8.

Table 3. Conductivity Values σ (S/cm) of Undoped and I_2-Doped P3HT and PCNCs

sample	undoped	doped
P3HT	2.85×10^{-5}	0.125
PCNC-1	6.4×10^{-4}	2.52
PCNC-2.5	4.9×10^{-5}	0.757
PCNC-8	3.56×10^{-3}	4.01

undoped state there is an increase of dc conductivity from 10^{-5} to 10^{-3} S/cm for the PCNC-8 sample. This may be explained by the red shift of the $\pi-\pi^*$ transition band of P3HT in the PCNCs. This decrease in band gap with increasing concentration of MWNT may result in the increase of intrinsic conductivity for the composites. On doping by iodine additional charge carriers are produced, increasing the conductivity to 0.125 S/cm for pure P3HT and 4.01 S/cm for PCNC-8. The small difference of conductivity value of pure P3HT than that reported earlier[24] might be due to the use of unfiltered samples, which also causes lower absorption maxima in the UV−vis spectra. It is noteworthy that there is a difference between the conductivity values of organically modified montmorillonite (omMMT)−clay nanocomposites and the MWNT−PCNCs of P3HT. In the former

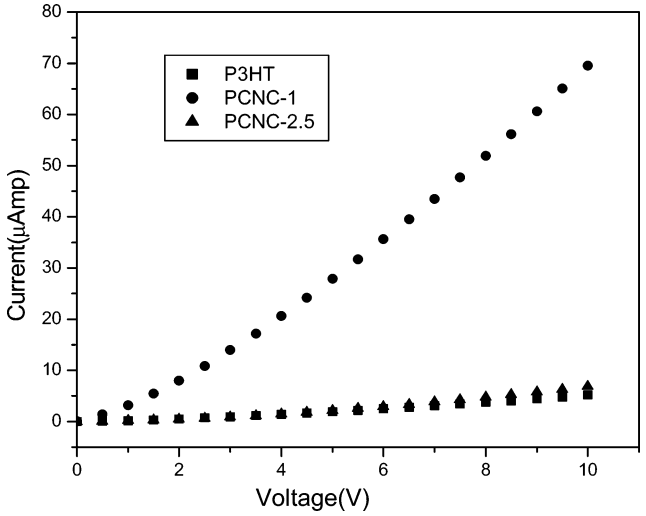

Figure 10. *I*−*V* characteristics of P3HT and different PCNCS.

case[24] there was practically no change in conductivity with increasing clay concentration in the undoped state, but in the latter composites there is a substantial increase of conductivity. This is because in the omMMT−P3HT nanocomposite the band gap has increased (blue shift in UV−vis spectra), but in the present case the band gap has decreased substantially (red shift in UV−vis spectra). In the PCNC-2.5 sample the conductivity values do not increase proportionally as that in the other two PCNCs probably due to the presence of the segregated phase of pure P3HT together with the wrapped P3HT on MWNT surface. In Figure 10 the *I*−*V* characteristic curves of the pure P3HT and the PCNCs are presented. From the figure it is apparent that pure P3HT and PCNC-2.5 have similar current−voltage (semiconducting) behavior, but the PCNC-1 has better semiconducting behavior. However, the *I*−*V* characteristic behavior of PCNC-8 sample could not be measured because of instrumental limitation to measure the high current on application of similar voltage.

Discussion

It is now worthy to discuss why the PCNC-2.5 sample exhibits different properties than the other PCNCs. The main cause is the presence of another phase of P3HT which have not wrapped the surface of MWNT. The reason may be the formation of very large molecular weight P3HT sample during in-situ preparation. MWNT comprises of sheets of large number of graphite units in two or more folds. It may therefore be imagined that MWNTs are rigid chain polymer with graphite units as monomeric units. Therefore, the miscibility of MWNT with the polymer may be qualitatively compared with the polymer−polymer miscibility. For the polymer−polymer miscibility specific interactions between the component polymer should exist.[54,55] But two chemically similar polymers may also mix if the similarity of the two components is very close to each other.[56] The small positive interaction between the components can be overcome by the entropy of mixing which is very small for the two component polymers. The mixing of MWNT with P3HT presumed to occur by the $\pi-\pi$ interaction between the conjugated double bond of graphite ring and conjugated double bond of P3HT.[38] The adsorption of P3HT and MWNT surface could also occur from CH$-\pi$ interactions.[14] The strength of such interactions are 1/10 of H-bonding interactions. In Figure 11 the FTIR spectra of CH stretching frequency region (∼2850 to 2916 cm^{-1}) of the P3HT and the

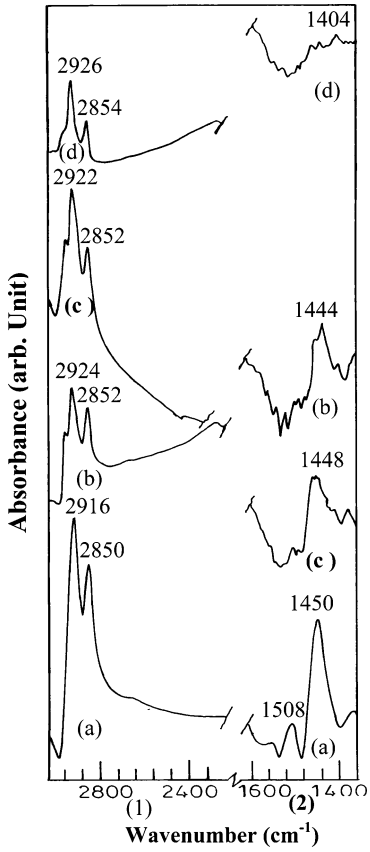

Figure 11. FT-IR spectra of P3HT and PCNCs at (1) CH stretching region and (2) ring stretching region of P3HT: (a) P3HT, (b) PCNC-1, (c) PCNC-2.5, and (d) PCNC-8.

PCNCs are shown. From the figure it is apparent that the CH (aliphatic) stretching frequency shows a shift to the higher frequency in all the PCNCs, suggesting the presence of CH$-\pi$ interaction in the system. In the figure the FTIR spectra relating to the presence of $\pi-\pi$ interaction between thiophene ring of P3HT and graphite unit of MWNT are presented. The 1510 and 1450 cm^{-1} peaks of P3HT correspond to the stretching vibration of thiophene ring.[57] In the PCNCs the 1510 cm^{-1} peak is not at all observed, and also the frequency of the 1415 cm^{-1} peak decreases to both in intensity and in peak position. This indicates that the stretching vibration of thiophene ring is reduced or modified in the mixture. This certainly indicates presence of $\pi-\pi$ interaction between graphite unit and the thiophene ring of polythiophene.[11,58] Further support for the presence of both $\pi-\pi$ and CH$-\pi$ interactions in the PCNCs can be obtained from the ^{1}H NMR spectra (Figure 12). The figure illustrates that the NMR peak of ring hydrogens (δ = 6.98 ppm) becomes broader in the PCNCs. This broadening may be attributed to the $\pi-\pi$ interactions between the thiophene ring and graphite ring of MWNT.[9,11] The NMR peaks of methylene protons of the pendent hexyl group (δ = 2.809, 2.579, 1.703, 1.567, 1.365 ppm) also broaden. Further, the CH_3 peak (0.916 ppm) shifts to somewhat upfield region (0.913 ppm) and also broadens in the PCNC samples. This indicates presence of molecular interaction between the pendent hexyl group and π cloud of MWNT,[9,11] and it may be attributed to CH$-\pi$ interaction. These are all dispersion interactions, and the amount of interaction is small and positive. But the process of mixing can occur if $\Delta G_m = \Delta H_m - T\Delta S_m$ is negative, indicating the entropy of mixing (ΔS_m) is the governing factor. MWNT has a rigid structure so the entropy

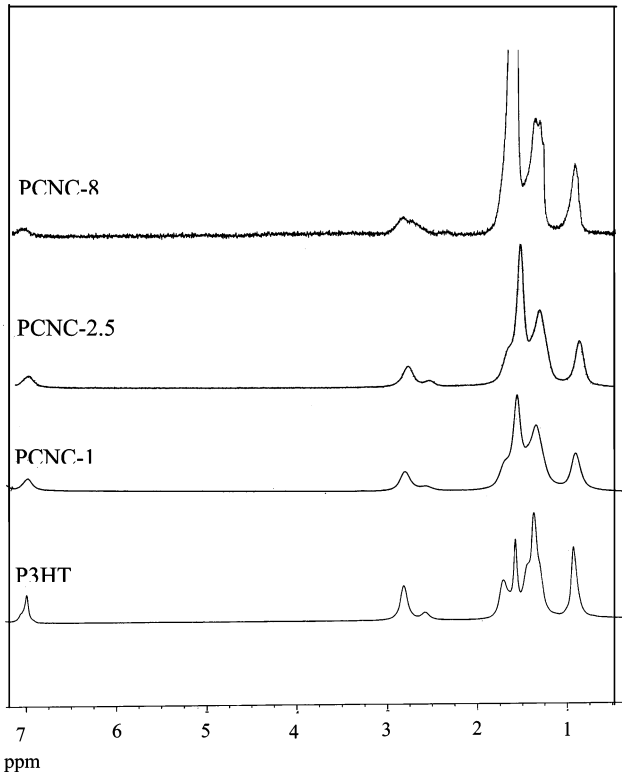

Figure 12. ^{1}H NMR spectra of P3HT and PCNC-1, PCNC-2.5, and PCNC-8 in $CDCl_3$.

of mixing with polymers cannot be exactly calculated from the Flory−Huggins expression for entropy of mixing of two polymers.[54,55]

$$\Delta S_m = -RN(\phi_1 \ln \phi_1/r_1 + \phi_2 \ln \phi_2/r_2) \qquad (2)$$

where $N = r_1n_1 + r_2n_2$, $\phi_1 = r_in_i/N$, r_i = number of segments of the *i*th component, and n_i = number of *i*th polymer molecules. Here we attempt to get an approximate picture of entropy of mixing using this equation and approximating polymer chainlike nature of MWNT. The $r_1$value of MWNT is considered to be 33 500,[59] and the r_2 values are calculated from the number-average molecular weight of the polymer. Considering 10 polymer molecules (n_2) are attached to a single carbon nanotube, the entropy of mixing per unit volume is calculated to be 1.09×10^{-3}, 0.98×10^{-3}, and 1.64×10^{-3} eu for PCNC-1, PCNC-2.5, and PCNC-8, respectively. This clearly indicates that with increase in molecular weight of P3HT the entropy of mixing decreases. So it may be argued that in the PCNC-2.5 the small +ve heat of mixing is not overcome by the entropy of mixing due to high molecular weight causing phase separation. However, in the TEM pictures we have observed some thickening of MWNT, and this might occur through the wrapping of lower molecular weight fraction of the polymer, as fractionation of low molecular weight polymer occurs during the phase separation process.[60] The temperature is also a governing factor in such a mixing process, and as temperature increases, the ΔG_m becomes more negative, causing homogeneous mixing. In our mechanical property discussion we have observed a fall of percent increase of storage modulus at 50 °C for PCNC-2.5, whereas in PCNC-1 and PCNC-8 it shows a large increase from those of 20 °C data (Table 2). The reason may be the ΔG_m value becomes negative at this temperature, favoring mixing between the phase-separated parts of PCNC2.5. This homogeneous mixture is responsible for the decrease of storage modulus compared to the increase in that of other two PCNCs at this temperature (Table 2). The almost unperturbed photoluminescence property and $I-V$ characteristics curve of the PCNC-2.5 (Figures 9 and 10) are probably due to the microphase separation of the P3HT in the composite. As in P3HT−clay nanocomposites,[24,25] the properties of melt-quenched PCNCs are expected to be somewhat different than that of the solvent-cast PCNCs and would be reported in a separate publication.

Conclusion

The MWNT−P3HT nanocomposites are prepared from the in-situ oxidative polymerization of 3-hexylthiophene in MWNT dispersion in $CHCl_3$ for different MWNT concentrations. The H−T regioregularity of P3HT is same in all PCNCs, but the molecular weight of PCNC-2.5 is very large ($\bar{M}_w = 2.02 \times 10^5$) compared to that of the P3HT in other PCNCs. TEM study indicates P3HT wraps MWNT well for PCNC-1, PCNC-2.5, and PCNC-8 samples, but in PCNC-2.5 apart from the wrapped MWNT there are some separate P3HT domains on the surface of wrapped MWNT. Probably, because of the very large molecular weight of P3HT it does not mix well with the MWNT, producing a separate phase of P3HT in the PCNC-2.5 sample. SEM study also corroborates the same observation as in TEM. The PCNCs in $CHCl_3$ produces a blackish-brown solution. The type I polymorph of P3HT is produced both in the pure P3HT and in the nanocomposites as evidenced from WAXS study. The melting point of P3HT in the PCNCs shows a marginal increase with increase in MWNT concentration, except for the PCNC-2.5 sample. Also, the degradation temperature of PCNCs has decreased compared to that of pure P3HT. The T_g of the P3HT remains the same in the PCNCs with that of pure P3HT, but T_β value changes differently for different compositions. Only the PCNC-2.5 sample exhibits two T_β values, indicating the existence of phase separation. The storage modulus of PCNCs has increased significantly compared to that of pure P3HT; the PCNC-8 exhibits a maximum of 158% increase at 50 °C. At lower temperature PCNC-2.5 exhibits a higher increment in G' than the other PCNCs probably due to the presence of the additional nanophase. But at 50 °C the increase is lowest for this composition, and mixing of the two phases has been attributed for such behavior. The UV−vis spectra of the composite film show a red shift of the $\pi-\pi^*$ transition band with increasing MWNT concentration, and the uncoiling of P3HT chain on the MWNT surface has been attributed for such behavior. But in the photoluminescence spectra there occurs a small blue shift due to the resonance stabilization of ground state through $\pi-\pi$ interaction. Further, there occurs fluorescence quenching with increase in MWNT concentration in the photoemission spectra though it is negligible for the PCNC-2.5 sample. The separate phase of P3HT in PCNC-2.5 might be a reason for the different behavior than that of PCNC-1 and PCNC-8 samples. FTIR and NMR studies indicate the presence of both CH$-\pi$ and $\pi-\pi$ interaction between P3HT and graphite unit of MWNT. In the PCNCs dc conductivity has increased by 2 orders than that of the pure P3HT in the undoped state, but in the doped state it has increased by 1 order. The PCNC-1 showed better semiconducting property in the $I-V$ plots than PCNC-2.5 and pure P3HT. The similar $I-V$ behavior of PCNC-2.5 with that of P3HT may be attributed to the presence of the separated nature of PCNC-2.5. Thus, the increased conductivity and mechanical property of P3HT in the easily processable MWNT−P3HT nanocomposite are interesting for its probable use in different optoelectronic appliances.

Acknowledgment. B. K. Kuila acknowledges the council of scientific and industrial research for granting a fellowship. The CSIR Grant 01-(1919)/04 EMR-II is gratefully acknowledged for financial support. Financial support from Department of Science and Technology Govt. of India, New Dehli, is gratefully acknowledged. We also gratefully acknowledge the help of Prof. C. Narayana, Jawaharlal Nehru Centre for Advanced Scientific Research, Bangalore, for Raman spectra of the MWNT sample.

Supporting Information Available: Figure S1 showing TEM pictures of PCNC-2.5 at different portions and Figure S2 showing TGA thermograms of P3HT and PCNCs. This material is available free of charge via the Internet at http://pubs.acs.org.

References and Notes

(1) Ajayan, P. M. *Chem. Rev.* **1999**, *99*, 1787.
(2) Baughman, R. H.; Zakhidov, A. A.; deHeer, W. A. *Science* **2002**, *297*, 787.
(3) Special Issue of Carbon Nanotubes. *Acc. Chem. Res.* **2002**, *35* (12).
(4) O'Connell, M. J.; Boul, P.; Ericson, L. M.; Huffman, C.; Wang, Y.; Haroz, E.; Kuper, C.; Tour, J.; Ausman, K. D.; Smalley, R. E. *Chem. Phys. Lett.* **2001**, *342*, 265.
(5) Tang, B. Z.; Xu, H. *Macromolecules* **1999**, *32*, 2569.
(6) Hughes, M.; Chen, G. Z.; Shaffer, M. S. P.; Fray, D. J.; Windle, A. H. *Chem. Mater.* **2002**, *14*, 1610.
(7) Bandyopadhyaya, R.; Nativ-Roth, E.; Regev, O.; Yerushalmi-Rozen, R. *Nano Lett.* **2002**, *2*, 25.
(8) Riggs, J. E.; Guo, Z.; Carroll, D. L.; Sun, Y.-P. *J. Am. Chem. Soc.* **2000**, *122*, 5879.
(9) Hill, D. E.; Lin, Y.; Rao, A. M.; Allard, L. F.; Sun, Y. P. *Macromolecules* **2002**, *35*, 9466.
(10) Ramasubramaniam, R.; Chen, J.; Liu, H. *Appl. Phys. Lett.* **2003**, *83*, 2928.
(11) Chen, J.; Liu, H.; Weimer, W. A.; Halls, M. D.; Waldeck, D. H.; Walker, G. C. *J. Am. Chem. Soc.* **2002**, *124*, 9034.
(12) Steuerman, D. W.; Star, A.; Narizzano, R.; Choi, H.; Ries, R. S.; Nicolini, C.; Stoddart, J. F.; Heath, J. R. *J. Phys. Chem. B* **2002**, *106*, 3124.
(13) Woo, H. S.; Czerw, R.; Webster, S.; Carroll, D. L.; Ballato, J.; Strevens, A. E.; O' Brien, D.; Blau, W. J. *Appl. Phys. Lett.* **2000**, *77*, 1393.
(14) Baskaran, D.; Mays, J. W.; Bratcher, M. S. *Chem. Mater.* **2005**, *17*, 3389.
(15) Jiang, X.; Bin, Y.; Matsuo, M. *Polymer* **2005**, *46*, 7418.
(16) Shaffer, M. S. P.; Koziol, K. *Chem. Commun.* **2002**, 2074.
(17) Wu, W.; Zhang, S.; Li, Y.; Li, J.; Liu, L.; Qin, Y.; Guo, Z.- X.; Dai, L.; Ye, C.; Zhu, D. *Macromolecules* **2003**, *36*, 6286.
(18) Liu, I.-C.; Huang, H.-M.; Chang, C.-Y.; Tsai, H.-C.; Hsu, C.-H.; Tsiang, R. C.-C. *Macromolecules* **2004**, *37*, 283.
(19) Cochet, M.; Maser, W. K.; Benito, A. M.; Callejas, M. A.; Martinez, M. T.; Benoit, J.- M.; Schreiber, J.; Chauvet, O. *Chem. Commun.* **2001**, 1450.
(20) Kong, H.; Gao, C.; Yan, D. *J. Am. Chem. Soc.* **2004**, *126*, 412.
(21) Zhao, B.; Hu, H.; Haddon, R. C. *Adv. Funct. Mater.* **2004**, *14*, 71.
(22) Roncali, J. *Chem. Rev.* **1992**, *92*, 711.
(23) McCullough, R. D.; Ewbank, P. C. In *Handbook of Conducting Polymers*, 2nd ed.; Skotheim, T. A., Elsenbaumer, R. L., Renolds, J. R., Eds.; Marcel Dekker: NewYork, 1998; p 225.
(24) Kuila, B. K.; Nandi, A. K. *Macromolecules* **2004**, *37*, 8577.
(25) Kuila, B. K.; Nandi, A. K. *J. Phys. Chem. B* **2006**, *110*, 1621.
(26) Pal, S.; Roy, S.; Nandi, A. K. *J. Phys. Chem. B* **2005**, *109*, 18332.
(27) Kabashi, M.; Takeuchi, H. *Macromolecules* **1998**, *31*, 7273.
(28) Yeh, J.-M.; Liou, S.-J.; Lai, C.-Y.; Wu, P.-C.; Tsai, T.-Y. *Chem. Mater.* **2001**, *13*, 1131.
(29) do Nascimento, G. M.; Constantino, V. R. L.; Landers, R.; Temperini, M. L. A. *Macromolecules* **2004**, *37*, 9373.
(30) Liu, Y.-C.; Tsai, C.-J. *Chem. Mater.* **2003**, *15*, 320.
(31) Kim, B.-H.; Jung, J.-H.; Hong, S.-H.; Joo, J.; Epstein, A. J.; Mizoguchi, K.; Kim, J. W.; Choi, H. J. *Macromolecules* **2002**, *35*, 1419.
(32) Bae, W. J.; Kim, K. H.; Jo, W. H.; Park, Y. H. *Macromolecules* **2004**, *37*, 9850.
(33) Curran, S. A.; Ajayan, P. M.; Blau, W. J.; Carroll, D. L.; Coleman, J. N.; Dalton, A. B.; Davey, A. P.; Drury, A.; McCarthy, B.; Maier, S.; Strevens, A. *Adv. Mater.* **1998**, *10*, 1091.
(34) Star, A.; Stoddart, J. F.; Steuerman, D.; Diehl, M.; Boukai, A.; Wong, E. W.; Yang, X.; Chung, S.-W.; Choi, H.; Heath, J. R. *Angew. Chem., Int. Ed.* **2001**, *40*, 1721.
(35) Sainz, R.; Benito, A. M.; Martinez, M. T.; Galindo, J. F.; Sotres, J.; Baro, A. M.; Corraze, B.; Chauvet, O.; Maser, W. K. *Adv. Mater.* **2005**, *17*, 278.
(36) Zengin, H.; Zhou, W.; Jin, J.; Czerw, R.; Smith, Jr, D. W.; Echegoyen, L.; Carroll, D. L.; Foulger, S. H.; Ballato, J. *Adv. Mater.* **2002**, *14*, 1480.
(37) Bhattacharyya, S.; Kymakis, E.; Amaratunga, G. A. J. *Chem. Mater.* **2004**, *16*, 4819.
(38) Kymakis, E.; Amaratunga, G. A. J. *Synth. Met.* **2004**, *142*, 161.
(39) Musa, I.; Baxendale, M.; Amaratunga, G. A. J.; Eccleston, W. *Synth. Met.* **1999**, *102*, 1250.
(40) Woo, H. S.; Czerw, R.; Webster, S.; Carroll, D. L.; Park, J. W.; Lee, J. H. *Synth. Met.* **2001**, *116*, 369.
(41) Malik, S.; Nandi, A. K. *J. Polym. Sci., Polym. Phys. Ed.* **2002**, *40*, 2073.
(42) Pavan Kumar, G. V.; Ashok Reddy, B. A.; Arif, M.; Kundu, T. K.; Narayana, C. *J. Phys. Chem. B* **2006**, *110*, 16787.
(43) Nemanish, R. J.; Solin, S. A. *Phys. Rev. B* **1979**, *20*, 392.
(44) Bin, Y.; Kitanaka, M.; Zhu, D.; Matsuo, M. *Macromolecules* **2003**, *36*, 6213.
(45) Chen, Q.; Bin, Y.; Matsuo, M. *Macromolecules* **2006**, *39*, 6528.
(46) Amou, S.; Haba, O.; Shirato, K.; HayaKawa, T.; Ueda, M.; Takeuchi, K.; Asai, M. *J. Polym. Sci., Polym. Chem.* **1999**, *37*, 1943.
(47) Ou, Y. Y.; Huang, M. H. *J. Phys. Chem. B* **2006**, *110*, 2031.
(48) Prosa, T. J.; Winokur, M. J.; McCullough, R. D. *Macromolecules* **1996**, *29*, 3654.
(49) Meille, S. V.; Romita, V.; Caronna, T.; Lovinger, A. J.; Catellani, M.; Belobrzeckaja, L. *Macromolecules* **1997**, *30*, 7898.
(50) Bolognesi, A.; Porzio, W.; Zhuo, G.; Ezquerra, T. *Eur. Polym. J.* **1996**, *32*, 1097.
(51) Gao, C.; Jin, Y. Z.; Kong, H.; Whitby, R. L. D.; Acquah, S. F. A.; Chen, G. Y.; Qian, H.; Hartschuh, A.; Silva, S. R. P.; Henley, S.; Fearon, P.; Kroto, H. W.; Walton, D. R. M. *J. Phys. Chem. B* **2005**, *109*, 11925.
(52) Ferry, J. D. *Viscoelastic Properties of Polymers;* John Wiley and Sons: New York, 1961.
(53) Malik, S.; Batabyal, S. K.; Basu, C.; Nandi, A. K. *J. Mater. Sci., Lett.* **2003**, *22*, 1113.
(54) Olabisi, O.; Robeson, L. M; Shaw, M. T. *Polymer-Polymer Miscibility*; Academic Press: NewYork, 1979.
(55) Paul, D. R., Newman, S., Eds. *Polymer Blends*; Academic Press: New York, 1978; Vols. I and II.
(56) Nandi, A. K.; Mandal, B. M.; Bhattacharyya, S. N. *Macromolecules* **1985**, *18*, 1454.
(57) Chen, T. A.; Wu, X.; Rieke, R. D. *J. Am. Chem. Soc.* **1995**, *117*, 233.
(58) Yang, D.-Q.; Rochette, J.-F.; Sacher, E. *J. Phys. Chem. B* **2005**, *109*, 4481.
(59) The number of graphite units in the MWNT has been computed by dividing the area of a cylinder of length 1000 Å, thickness 70 Å by the area of a graphite unit = 6.56 Å^2. The number of graphite units comes to be 67 000. In the calculation of eq 1 we are taking r_1= 33 500 considering only the upper part of the tube is involved in the mixing process.
(60) Flory, P. J. *Principles of Polymer Chemistry*; Cornell University Press: Ithaca, NY, 1953.

MA061548E